Chinese Chemical Letters 37 (2026) 111450

Contents lists available at ScienceDirect

Chinese Chemical Letters

journal homepage: www.elsevier.com/locate/cclet

Cisplatin-polyphenol complex liposomes reduce chemotherapy toxicity

Yizhi Ge[a,1], Jiahui Zou[b,1], Hui Liu[b,1], Wei He[b,*], Huanfeng Zhu[a,*]

[a] Department of Radiation Oncology, Jiangsu Cancer Hospital & Jiangsu Institute of Cancer Research & The Affiliated Cancer Hospital of Nanjing Medical University, Nanjing 210009, China
[b] School of Pharmacy, China Pharmaceutical University, Nanjing 211198, China

ARTICLE INFO

Article history:
Received 10 April 2025
Revised 11 June 2025
Accepted 12 June 2025
Available online 12 June 2025

Keywords:
Cisplatin
Polyphenolic substances
CDDP-polyphenol complex
Liposome
Toxic side effect

ABSTRACT

Cisplatin (CDDP)-based chemotherapy is an effective strategy for the treatment of advanced nasopharyngeal carcinoma (NPC). However, serious toxic side effects of CDDP limit patient tolerance and treatment compliance, which urgently needs to be addressed in clinical application. Liposomes have been considered ideal vehicles for reducing CDDP toxicity due to their high biocompatibility, low toxicity and passive targeting ability. Nevertheless, CDDP's poor water/lipid solubility usually results in a low liposome drug-lipid ratio, limiting tumor delivery ability. Herein, a CDDP-polyphenol complex liposome was designed to increase the drug loading capacity of CDDP to realize the reduction of toxicity and effective antitumor effect simultaneously. The complex was prepared *via* complexation reaction of different stoichiometric ratios of CDDP and polyphenolic substances (gallic acid, epigallocatechin gallate and tannic acid), followed by encapsulation of complex in liposomes to improve tumor targeting. Notably, the molecular interaction forces between CDDP and polyphenolic substances were intensively investigated through a binding force disruption assay. *In vitro* studies demonstrated that the optimal formulation of CDDP-epigallocatechin gallate complex liposome (CDDP-EGCG Lips) showed the highest CDDP encapsulation efficiency, favorable stability, pH-sensitive release, enhanced cellular uptake and apoptosis effect. *In vivo* studies revealed that CDDP-EGCG Lips retarded the elimination of CDDP to prolong their circulation time, inhibited the growth of tumors, and significantly reduced the toxic side effects compared to CDDP monotherapy. This delivery strategy holds great promise for improving the clinical use of platinum-based drugs.

© 2025 Published by Elsevier B.V. on behalf of Chinese Chemical Society and Institute of Materia Medica, Chinese Academy of Medical Sciences.

Nasopharyngeal carcinoma (NPC) is one of the most common malignant tumors of the head and neck and has become a severe worldwide malignant disease threatening human health [1]. Due to the insidious site of onset, about 75% of patients are in locally advanced stages at the time of first consultation [2]. Cisplatin (CDDP)-based therapy is effective in combatting the advanced NPC [3]. However, clinical practice has shown that CDDP chemotherapy can trigger severe toxic side effects, including renal toxicity, peripheral nerve injury, myelosuppression, ototoxicity, nausea and vomiting, *etc.* [4]. Several clinical studies have indicated that more than one-third of patients on concurrent radiotherapy were unable to complete three cycles of concurrent CDDP chemotherapy [5]. Therefore, despite the significant efficacy of CDDP in the treatment of NPC, severe toxic side effects significantly limit patient tolerance and treatment adherence, which has become a key issue that needs to be solved with strategies in clinical treatment [6].

Liposomes (Lips) have been well-recognized as vital drug delivery systems and are widely used in oncotherapy [7,8]. Due to the structure of the phospholipid bilayer and hydrophilic inner cavity, Lips can load both hydrophilic and hydrophobic drugs [9,10]. Importantly, favorable properties, such as high biocompatibility, low toxicity, passive targeting ability, *etc.*, have led to the widespread application of Lips for encapsulating drug candidates for reducing toxicity and extending the duration of therapeutic effect [11]. Therefore, these advantages make Lips synthetically recognized as ideal delivery carriers for reducing severe toxic side effects caused by CDDP chemotherapy [12]. However, CDDP is poorly water/lipid-soluble, resulting in inefficient Lip encapsulation, limiting the effective CDDP delivery to tumors and therapeutic outcomes [13]. Thus, further combining other technologies to improve CDDP delivery for effective anti-NPC chemotherapy is necessary.

Polyphenolic compounds are naturally occurring compounds derived from plants found in everyday life, often characterized by polyhydroxy structures [14,15]. In their structures, the catechol and pyrogallol groups can be complex with various metal ions, including platinum, iron manganese, *etc.*, to form coordination complexes [16,17]. Primarily, the Pt(II) center in CDDP preferentially coordi-

* Corresponding authors.
E-mail addresses: weihe@cpu.edu.cn (W. He), zhuhuanf@njmu.edu.cn (H. Zhu).
[1] These authors contributed equally to this work.

https://doi.org/10.1016/j.cclet.2025.111450
1001-8417/© 2025 Published by Elsevier B.V. on behalf of Chinese Chemical Society and Institute of Materia Medica, Chinese Academy of Medical Sciences.

nates with two adjacent electron-donating groups to form stable chelate rings, with the catechol structure being the most favorable due to high complexation stability [18]. Several polyphenolic compounds, such as gallic acid (GA), epigallocatechin gallate (EGCG) and tannic acid (TA), demonstrate catechol structure with promising safety and are often used as complexation candidates [19]. This strategy of preparing the platinum-polyphenol complex can significantly increase the water solubility of platinum drugs and modify their physicochemical properties, simultaneously improving the encapsulation efficiency of platinum-based medications in Lips [20,21]. In addition, the complexation of platinum drugs by polyphenols to form complexed nanoparticles can also reduce the systemic toxicity of platinum drugs without altering their antitumor activity [22]. Therefore, screening CDDP with different kinds of polyphenols to construct a complex is a promising approach to improve the encapsulation efficiency of CDDP in Lips for combined enhancement of therapeutic efficacy and toxicity reduction [23].

In this study, we prepared CDDP-polyphenol complex Lip for effective treatment of NPC, especially reducing the toxic side effects induced by single-CDDP chemotherapy. We first prepared and characterized various CDDP-polyphenol complexes for different types of polyphenolic substances (GA, EGCG, and TA) and CDDP: polyphenol ratios. Especially, we confirmed the molecular interaction forces between CDDP and different polyphenolic substances through binding force disruption assay by incubating with EDTA, KNO_3, Tween 20 and CH_4N_2O, respectively. Then, CDDP-polyphenol complex Lips were prepared and characterized to optimize the formulation. A pharmacokinetic study was also conducted to evaluate the *in vivo* behavior of CDDP-EGCG Lips. Importantly, we established a CNE-2 NPC tumor model to investigate *in vivo* antitumor effects and biosafety of the preparations. CDDP-polyphenol complex Lips reduced the toxic side effects of CDDP and were effective in combating tumors, demonstrating the potential to improve the clinical application of platinum-based drugs for chemotherapy.

First, different CDDP-polyphenol complexes were prepared by CDDP and three types of polyphenolic substances (GA, EGCG and TA), and characterized with particle size and polydispersity index (PDI) [24]. All three CDDP-polyphenol complexes (CDDP-GA, CDDP-EGCG and CDDP-TA) showed favorable dispersibility with uniform particle size distribution (Table S1 in Supporting information). Then, the preparation of the CDDP-polyphenol complex was confirmed *via* the ultraviolet-visible spectroscopy (UV–vis) method. Compared to the polyphenol solution, three CDDP-polyphenol complexes all exhibited red-shift in the E2 band, which may be due to the complexation of CDDP with polyphenols increased the co-planarity of atoms and groups in the molecule (Figs. 1A–C). Three CDDP-polyphenol complexes were incubated with EDTA, KNO_3, Tween 20 and CH_4N_2O to investigate further molecular interactions between CDDP and polyphenolic substances (GA, EGCG and TA), respectively (Figs. 1D–O). As reported, EDTA, KNO_3, Tween 20 and CH_4N_2O can destroy coordinate bonds, ionic bonds, hydrophobic interaction and hydrogen bonds in complex, respectively [25–28]. In the CDDP-GA complex, UV–vis scanning results demonstrated that the interactions between CDDP and GA were mainly coordinate and ionic bonds. In the CDDP-TA complex, the interactions between CDDP and TA were mainly coordinate bonds, ionic bonds, and hydrophobic interactions. In the CDDP-EGCG complex, the interactions between CDDP and EGCG were mainly coordinate and ionic bonds.

Then, the CDDP loading efficiency of CDDP-polyphenol complex was investigated at different CDDP: polyphenol ratios (2:1, 3:1 and 5:1). The complex of CDDP-GA, CDDP-TA and CDDP-EGCG had the highest drug loading efficiency at the 2:1 ratio, demonstrating 56.88% ± 5.18% (Fig. S1 in Supporting information), 79.4% ± 1.02% (Fig. S2 in Supporting information) and 78.96% ± 5.21% (Fig. S3 in Supporting information), respectively. Especially, the CDDP-TA/CDDP-EGCG complex showed a significantly higher loading efficiency than the CDDP-GA complex, possibly due to the increasing phenolic hydroxyl reactive groups reacting with CDDP on TA and EGCG in their structures [29].

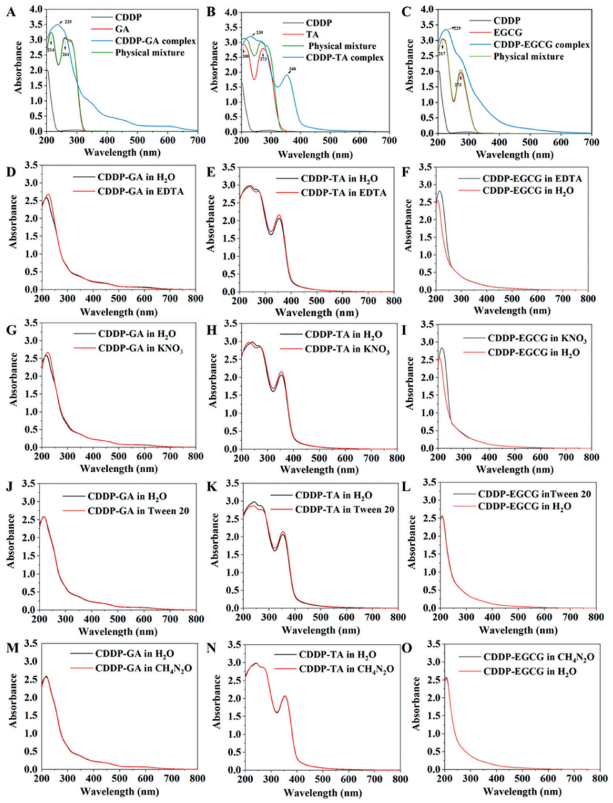


Fig. 1. Preparation and characterization of CDDP-polyphenol complex. UV scanning spectrum of CDDP-polyphenol complex prepared by CDDP with (A) GA, (B) TA and (C) EGCG. Evaluation of coordinate bond in CDDP-polyphenol complex *via* incubation of EDTA with (D) CDDP-GA, (E) CDDP-TA and (F) CDDP-EGCG. Evaluation of ionic bond in CDDP-polyphenol complex *via* incubation of KNO_3 with (G) CDDP-GA, (H) CDDP-TA and (I) CDDP-EGCG. Evaluation of hydrophobic interaction in CDDP-polyphenol complex *via* incubation of tween-20 with (J) CDDP-GA, (K) CDDP-TA and (L) CDDP-EGCG. Evaluation of hydrogen bond in CDDP-polyphenol complex *via* incubation of CH_4NO_2 with (M) CDDP-GA, (N) CDDP-TA and (O) CDDP-EGCG.

CDDP-polyphenol complex Lips were prepared *via* the reverse evaporation method. We first optimized the formulation of CDDP-polyphenol complex Lips by the encapsulation rate of CDDP through the type of polyphenols, CDDP: phospholipid ratios (w/w), CDDP: cholesterol ratios (w/w), organic-phase: aqueous phase ratios (v/v), *etc*. As shown in Fig. 2A, the CDDP encapsulation rate of CDDP-EGCG Lips was higher than CDDP-GA Lips and CDDP-TA Lips, indicating that EGCG improved the encapsulation efficiency. Then, we investigated the effect of CDDP:cholesterol ratio (w/w) on particle size and encapsulation. CDDP-EGCG Lips exhibited moderate particle size and the highest encapsulation rate of CDDP when the CDDP:cholesterol ratio was set as 1:10 (Fig. 2B). Furthermore, when the ratio (w/w) was 5:1 (Fig. 2C) and the organic-phase: aqueous phase ratio (v/v) was 2:1 (Fig. S4 in Supporting information), CDDP-EGCG Lips exhibited the smallest particle size and highest encapsulation efficiency among the formulations. The optimized Lips had a CDDP loading of 4.16% (w/w). Two CDDP-loaded Lips (Lipoplatin® and SPI-77) under clinical investigation load 9.1% and 1.4%, respectively. However, Lipoplatin® requires a technically complex preparation process, including precisely controlling pH and ionic strength to form reverse micelles and subsequent conversion into Lips initially. In contrast, CDDP-EGCG Lips were prepared

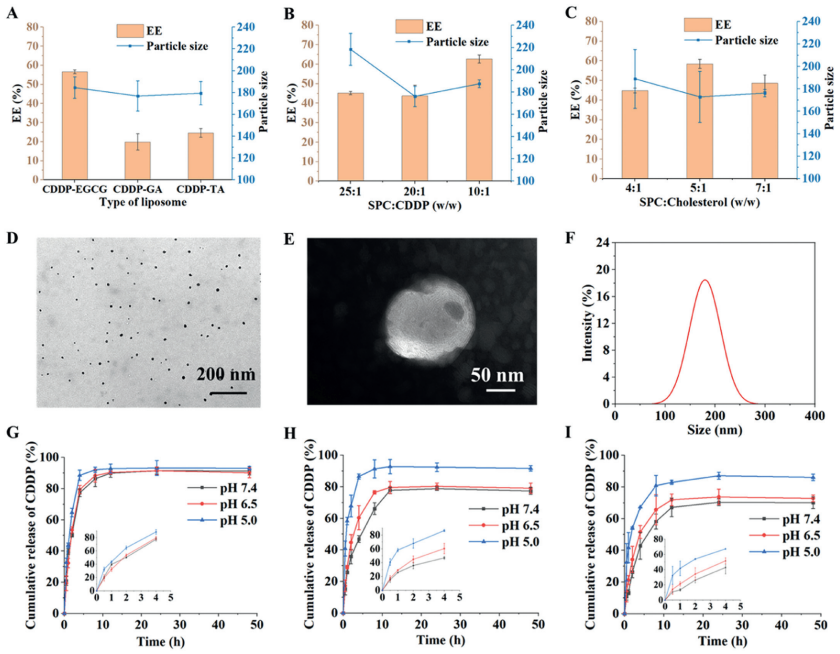


Fig. 2. Preparation and characterization of CDDP-EGCG Lips. (A) Encapsulation efficiency and particle size of CDDP-EGCG Lips, CDDP-GA Lips and CDDP-TA Lips. Optimization of (B) SPC:CDDP ratio (w/w) and (C) SPC:cholesterol ratio (w/w) for preparation of CDDP-EGCG Lips. (D) Transmission electron microscope (TEM) images of CDDP-EGCG complex. Scale bar: 200 nm. (E) TEM image and (F) particle size distribution profiles of CDDP-EGCG Lips. Scale bar: 50 nm. *In vitro* release of (G) CDDP, (H) CDDP-EGCG complex and (I) CDDP-EGCG Lips under different pH conditions (pH 5.0, 6.5 and 7.4). Data are presented as mean ± SD ($n = 3$).

using reverse-phase evaporation, a well-established and technically straightforward preparation protocol.

According to transmission electron microscope observation, CDDP-EGCG complex (Fig. 2D) and CDDP-EGCG Lips (Fig. 2E) showed uniform spherical morphology. The particle size, PDI, and zeta potential of the optimal CDDP-EGCG Lips formulation were 152.46 ± 4.50 nm, 0.268 ± 0.011, and −38.34 ± 0.15 mv, respectively (Fig. 2F and Table S2 in Supporting information). *In vitro* release of preparations was conducted under different pH conditions (pH 5.0, 6.5 and 7.4). CDDP demonstrated similar release behavior under various pH conditions (Fig. 2G) [30]. Differently, the release of CDDP-EGCG (Fig. 2H) and CDDP-EGCG Lips (Fig. 2I) was pH-responsive, with a slower release rate at physiological conditions (pH 7.4) and accelerated drug release under acidic conditions. This pH-sensitive release was attributed to the phenolic hydroxyl groups in polyphenols. They underwent deprotonation ($-O^-$), forming stable coordination bonds with Pt(II) [31]; while in acidic environments, the protonation of hydroxyl groups ($-OH_2^+$) reduced their electron density weakening Pt coordination and promoted drug release through complex dissociation. These results suggested that CDDP could remain stable in the circulation and rapidly release CDDP at the tumor site, leading to reduced systemic toxicity. A 28-day storage under 4 °C did not significantly change the particle size and CDDP encapsulation efficiency of the CDDP-EGCG complex (Fig. S5A in Supporting information) and CDDP-EGCG Lips (Fig. S5B in Supporting information), indicating their promising stability for application. CDDP-EGCG Lips demonstrated little changes in the particle size and PDI after incubation with 10 % serum-containing phosphate buffer saline (PBS) at 37 °C for 12 h and, as a result, potential stability against disassociation (Fig. S6 in Supporting information).

Next, we studied the *in vitro* antitumor effect of preparations. As shown in Figs. 3A and B, the blank Lip demonstrated little influence on cell viability of both CNE-2 and 5–8F cells under the experimental concentration range, indicating that the carrier had good biocompatibility and biosafety. The CDDP-loading preparations, free CDDP, CDDP-EGCG complex and CDDP-EGCG Lips, ex-

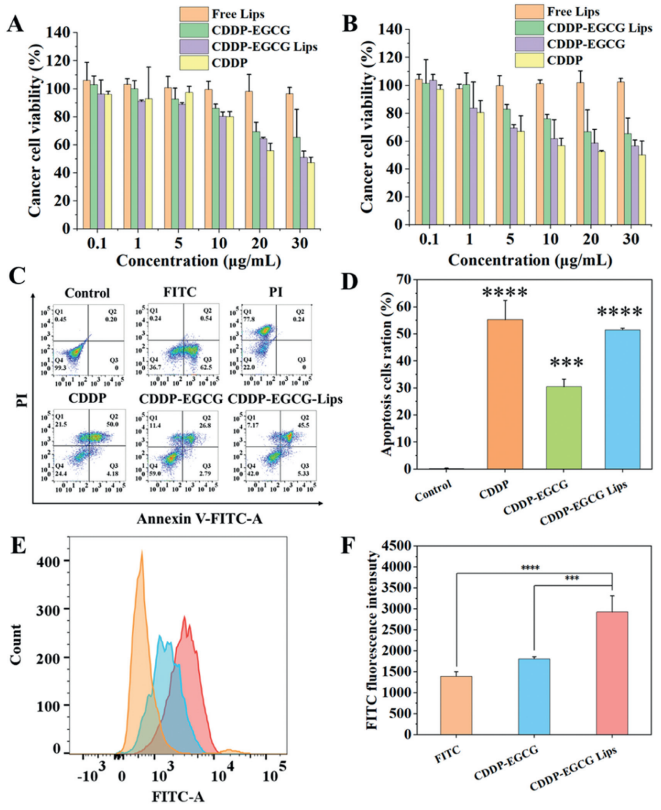


Fig. 3. *In vitro* antitumor effects. Cytotoxicity of free Lips, CDDP, CDDP-EGCG and CDDP-EGCG Lips for CNE-2 and 5–8F cells under the CDDP concentration of 0.1, 1, 5, 10, 20 and 30 μg/mL. (C) Representative flow cytometry image and (D) quantitative analysis of FITC, FITC–CDDP-EGCG and FITC–CDDP-EGCG Lips after cellular uptake by CNE-2 cells. (E) Representative flow cytometry images and (F) quantitative analysis for cell apoptosis evaluation of CNE-2 cells after treatment with CDDP, CDDP-EGCG and CDDP-EGCG Lips. $^{***}P < 0.001$, $^{****}P < 0.0001$. Data are presented as mean ± SD ($n = 5$).

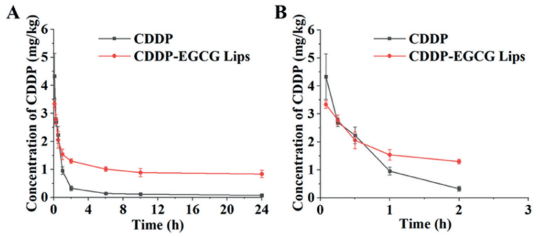


Fig. 4. Pharmacokinetic study of CDDP and CDDP-EGCG Lips. Blood retention curves of CDDP and CDDP-EGCG Lips for (A) 24 h and (B) 3 h *via* ICP-MS detection. Data are presented as mean ± SD ($n = 5$).

hibited significant dose-dependent cytotoxicity against both tumor cells. When the drug concentration reached 30 μg/mL, the survival rate of CNE-2 cells and 5–8F cells was nearly 50 %. All three formulations showed potent antitumor activity on CNE-2 and 5–8F tumor cells, with comparable inhibitory effects. Then, we investigated the ability of preparations to induce apoptosis of CNE-2 cells. The three preparations significantly induced apoptosis of CNE-2 cells compared to the untreated negative control group (Figs. 3C and D). Specifically, the total percentage of early and late apoptotic cells in the CDDP-EGCG Lip-treated group was 51.5 % ± 0.59 %, comparable to the CDDP-treated group 55.33 % ± 7.08 %. In addition, the apoptosis fluorescence images of CNE-2 cells demonstrated that CDDP, CDDP-EGCG complex and CDDP-EGCG Lips induced shrinkage and nuclear chromatin condensation of CNE-2 cells, suggesting the occurrence of tumor cell apoptosis (Fig. S7 in Supporting information). These results indicated that CDDP-EGCG Lips could effectively induce apoptosis on tumor cells, similar to CDDP. The enhanced proapoptotic effect of the preparation was due to the effective drug cellular uptake. As depicted in Figs. 3E and F, the fluorescein isothiocyanate (FITC) fluorescence intensity of the CDDP-EGCG-FITC Lips group was significantly higher compared to CDDP-EGCG-FITC ($P < 0.0001$).

Finally, we studied the *in vivo* performance of the preparations. All animal experimental procedures were approved by the Ethics Committee of China Pharmaceutical University (approval No. 202406068). First, the pharmacokinetics were evaluated within 24 h on Sprague-Dawley rats. The plasma concentration of CDDP was detected *via* inductively coupled plasma mass spectrometry (ICP-MS) [32]. Remarkably, under the same dose of CDDP administration, CDDP-EGCG Lips significantly delayed elimination and prolonged the circulation of CDDP than single CDDP administration (Figs. 4A and B and Table S3 in Supporting information), demonstrating an approximately 10-fold increase in the elimination half-life and 4-fold increase in bioavailability. The improved *in vivo* behavior of CDDP by the Lips could facilitate the delivery of CDDP to tumor sites and decrease accumulation in normal tissues, effectively combating cancer and reducing toxic side effects. Moreover, the significantly prolonged *in vivo* circulation and improved bioavailability of CDDP-EGCG Lips could prolong the action duration and reduce the frequency of administration in clinical applications.

Then, the *in vivo* pharmacodynamic study of CDDP, CDDP-EGCG complex and CDDP-EGCG Lips on CNE-2 tumor-bearing mice (Fig. S8 in Supporting information). As shown in Figs. 5A–C, compared to the control (saline) group, the preparation treatment using CDDP, CDDP-EGCG complex and CDDP-EGCG Lips significantly inhibited tumor growth after 13-day treatment, with the CDDP group and CDDP-EGCG Lips group showing higher tumor growth inhibition. The immunohistochemical staining displayed that the percentage of Ki-67-positive cells in tumor tissues in the control group was 12.71 % ± 1.83 %, while the Ki-67-positive rates in the groups treated using the three preparations were 6.59 % ± 0.84 %,

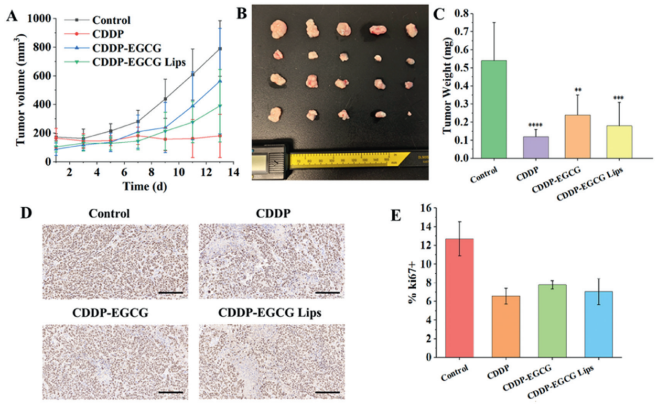


Fig. 5. *In vivo* antitumor efficiency. (A) Tumor growth profiles, (B) tumor images and (C) tumor weight of CNE-2 tumor-bearing mice after treatment. (D) Ki67 staining and (E) quantitative analysis of tumor tissues. Scale bar: 100 μm. $^{*}P < 0.05$, $^{**}P < 0.01$, $^{***}P < 0.001$. Data are presented as mean ± SD ($n = 5$).

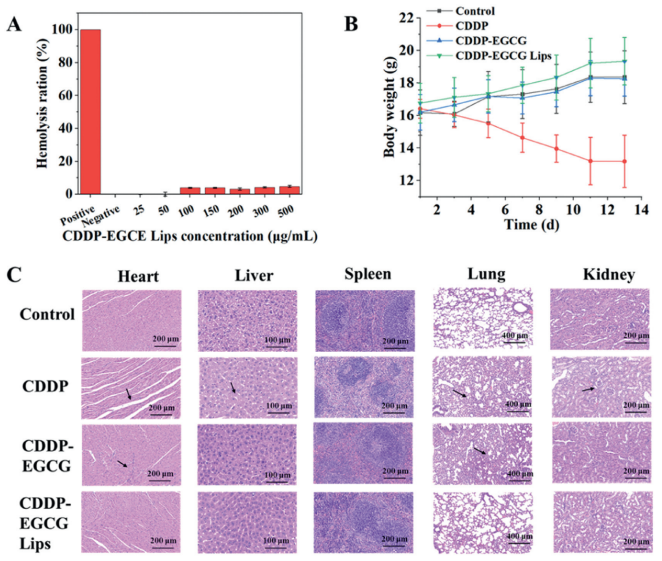


Fig. 6. Safety evaluation and reduced chemotherapy toxicity of CDDP-EGCG Lips. (A) Hemolysis evaluation of CDDP-EGCG Lips under several concentrations. (B) The body weight of CNE-2 tumor-bearing mice within 13 days. (C) Hematoxylin-eosin (HE) staining of heart, liver, spleen, lung, and kidney tissue sections at the end of continuous treatment. Scale bar: 200 μm (heart), 100 μm (liver), 200 μm (spleen), 400 μm (lung) and 200 μm (kidney), respectively. Data are presented as mean ± SD ($n = 5$).

7.80 % ± 0.44 % and 7.04 % ± 1.40 %, respectively (Figs. 5D and E). The results indicated that CDDP-EGCG Lips effectively inhibited the proliferation of tumor cells.

We also investigated the biosafety of the preparations. *In vitro* hemolysis examination demonstrated that CDDP-EGCG Lips did not cause significant hemolysis even at a high CDDP concentration of 500 μg/mL, indicating favorable blood compatibility and non-significant damage to erythrocytes (Fig. 6A) [33]. Then, we monitored the body weight changes during the treatment period in each group of mice to assess the systemic toxicity of different dosing regimens to mice [34]. Mice in the CDDP group showed significant body weight loss after administration, suggesting that CDDP monotherapy has substantial systemic toxicity. In contrast, the body weight of mice in the CDDP-EGCG Lips group maintained a normal growth trend, with non-significant alteration compared to the control group, indicating remarkable biosafety (Fig. 6B). Organ pathological changes showed that CDDP had strong toxic effects on several organ tissues, and no significant tissue damage

was seen in the CDDP-EGCG Lips group, with a good safety profile (Fig. 6C). This enhanced biosafety and reduced systemic toxicity mainly because the CDDP-EGCG Lips could enhance tumor accumulation of CDDP and reduce drug distribution in normal tissues. Moreover, the pH-sensitive release of CDDP-EGCG Lips could compromise drug release in normal tissues and minimize toxicity to the body. CDDP-EGCG Lips were capable of rapidly releasing CDDP in response to the acidic condition in tumor microenvironment (pH 6.0–7.0) and endosome-lysosomes (pH 4.0–5.0), while remaining stable in the near-neutral condition in normal tissues (pH 7.2–7.4) to reduce CDDP accumulation and decrease toxic side effects [35,36].

In summary, to address the shortcomings in the clinical chemotherapy of CDDP, we developed a CDDP-polyphenol complex Lip nanoplatform. We first screened different kinds of polyphenol compounds and drugs, such as polyphenol ratios, to prepare a CDDP-polyphenol complex with high CDDP-loading efficiency, effectively improving the poor water/lipid solubility properties of CDDP. The optimal CDDP-EGCG complex was further encapsulated in Lips by reverse evaporation to enhance their biosafety, prolong *in vivo* circulation, and improve tumor accumulation. The CDDP-EGCG Lips could dramatically alleviate the toxic side effects caused by CDDP chemotherapy and significantly enhance the drug's safety while ensuring the antitumor efficacy. In addition, this drug-polyphenol-Lip strategy has great potential to be applied to other cancer chemotherapy medicines, aiming to reduce toxic side effects and improve therapeutic efficacy.

Declaration of competing interest

The authors declare that they have no known competing financial interests or personal relationships that could have appeared to influence the work reported in this paper.

CRediT authorship contribution statement

Yizhi Ge: Writing – original draft, Validation, Resources, Methodology, Investigation. **Jiahui Zou:** Writing – original draft, Validation, Resources, Methodology, Investigation. **Hui Liu:** Writing – original draft, Validation, Resources, Methodology, Investigation. **Wei He:** Writing – review & editing, Supervision, Resources, Funding acquisition, Conceptualization. **Huanfeng Zhu:** Writing – review & editing, Supervision, Resources, Funding acquisition, Conceptualization.

Acknowledgments

This study was supported by the National Natural Science Foundation of China (Nos. 81872823, 82073782, and 82241002) and the Key R&D Plan of Ganjiang New District of Jiangxi (No. 2023010).

Supplementary materials

Supplementary material associated with this article can be found, in the online version, at doi:10.1016/j.cclet.2025.111450.

References

[1] K.C. Wong, E.P. Hui, K.W. Lo, et al., Nat. Rev. Clin. Oncol. 18 (2021) 679–695.
[2] H. Wang, T. Fan, Y. Lu, et al., Int. J. Cancer 157 (2025) 239–250.
[3] L. Xie, F. Shi, Y. Li, et al., Signal. Transduct. Target. 5 (2020) 56.
[4] U. Anand, A. Dey, A.K.S. Chandel, et al., Genes. Dis. 10 (2023) 1367–1401.
[5] N. Riaz, E. Sherman, L. Koutcher, et al., Am. J. Clin. Oncol. Canc. 39 (2016) 27–31.
[6] A. Lee, J.C. Chow, N.Y. Lee, JAMA Oncol. 7 (2021) 445–453.
[7] R. Liu, C. Luo, Z. Pang, et al., Chin. Chem. Lett. 34 (2023) 107518.
[8] X. Li, Y. Lai, G. Wan, et al., Chin. J. Nat. Med. 22 (2024) 1100–1116.
[9] S. Dadashzadeh, N. Mirahmadi, M. Babaei, et al., J. Control. Release 148 (2010) 177–186.
[10] X. Li, J. Gu, Q. Xiao, et al., Chin. Chem. Lett. 34 (2023) 107483.
[11] X. Wang, C. Li, Y. Wang, et al., Acta Pharm. Sin. B 12 (2022) 4098–4121.
[12] J.A. Santos, D. Silva, M.P.M. Marques, Nanoscale 16 (2024) 14640–14686.
[13] H. Liu, J. Zou, X. Li, Y. Ge, W. He, J. Control. Release 380 (2025) 503–523.
[14] M. Abbas, F. Saeed, F.M. Anjum, et al., Int. J. Food. Prop. 20 (2017) 1689–1699.
[15] B. Li, C. Teng, H. Yu, et al., Acta Pharm. Sin. B 13 (2023) 2369–2382.
[16] H. Geng, Q. Zhong, J. Li, et al., Chem. Rev. 122 (2022) 11432–11473.
[17] K.T. Magar, G.F. Boafo, M. Zoulikha, et al., Chin. Chem. Lett. 34 (2023) 107453.
[18] J. Xiang, Y. Li, Y. Zhang, et al., J. Control. Release 330 (2021) 992–1003.
[19] X. Zhang, Z. Li, P. Yang, et al., Mater. Horiz. 8 (2021) 145–167.
[20] Y. Guo, Q. Sun, F.G. Wu, et al., Adv. Mater. 33 (2021) 2007356.
[21] X. Wang, Z. Guo, Chem. Soc. Rev. 42 (2013) 202–224.
[22] Y. Chen, C. Chen, X. Zhang, et al., Acta Pharm. Sin. B 10 (2020) 1106–1121.
[23] Y. Dai, S. Cheng, Z. Wang, et al., ACS Nano 12 (2018) 455–463.
[24] Z. Ren, S. Sun, R. Sun, et al., Adv. Mater. 32 (2020) 1906024.
[25] L. Chen, T. Liu, C.a. Ma, J. Phys. Chem. A 114 (2010) 443–454.
[26] W. Xie, Z. Zhang, Y. Gao, J. Phys. Chem. B 120 (2016) 2343–2351.
[27] X. Xin, H. Zhang, G. Xu, et al., Colloid. Surface. A 418 (2013) 60–67.
[28] C. Xin, J. Chen, H. Liang, et al., Carbohyd. Polym. 174 (2017) 337–342.
[29] Z. Zhang, L. Xie, Y. Ju, et al., Small 17 (2021) 2100314.
[30] J. Peng, T. Qi, J. Liao, et al., Biomaterials 34 (2013) 8726–8740.
[31] J. Xiang, Y. Zhang, X. Liu, et al., Nano Lett. 22 (2022) 5615–5625.
[32] C.J. Greenhalgh, E. Karekla, G.J. Miles, et al., Anal. Chem. 92 (2020) 9847–9855.
[33] N. Rani, K. Rawat, M. Saini, et al., ACS Omega 8 (2023) 14509–14519.
[34] X. Chen, F. Meng, Y. Xu, et al., Nat. Commun. 14 (2023) 4584.
[35] H. Ding, P. Tan, S. Fu, et al., J. Control. Release 348 (2022) 206–238.
[36] Y. Park, S. Kwon, G. Lee, et al., J. Control. Release 330 (2021) 1–14.